# LWA Rate Adaption by Enhanced Event-Triggered Reporting

Yi-Bing Lin, *Fellow, IEEE*, Ying-Ju Shih, Hung-Chun Tseng, and Ling-Jyh Chen

***Abstract*—Unlicensed spectrum has been utilized to open up additional capacity to support long-term evolution (LTE) service. LTE and wireless local area network (WLAN) Aggregation (LWA) is a perfect solution that satisfies this need. In 2017, Taiwan has deployed the first commercial LWA service. The deployed LWA network reuses and is nicely merged with the existing individual LTE and WLAN networks. To provide appropriate WLAN transmission bandwidth, the user equipment periodically measures the WLAN quality and reports the results to the eNB (the LTE base station). The eNB then decides if the transmission rate should be adapted. We investigate the performance of periodical reporting and then propose the enhanced event-triggered reporting to improve the performance of WLAN transmission rate adaption. We suggest how to select appropriate frequency to minimize the network traffic of periodical reporting. We also show that enhanced event-triggered reporting outperforms periodical reporting. Our solution utilizes the standard 3GPP protocols and does not modify the mobile phone's software.**

***Index Terms*—Long term evolution (LTE), wireless local area network (WLAN), LTE and WLAN aggregation (LWA), measurement report, unlicensed spectrum, Wi-Fi.**

## I. Introduction

IN THE recent years, mobile users and mobile data traffic have been dramatically increased, the telecom operators are seeking solutions to support more users and wider bandwidth including device-to-device communications [18], [19], Licensed Assisted Access (LAA) [22], and LTE and WLAN Aggregation (LWA) [7]. Both LAA and LWA utilize unlicensed spectrum to open up additional Long Term Evolution (LTE) service capacity. Since most wireless data is consumed indoors, unlicensed spectrum is particularly suited to indoor deployments, which is a key market for mobile operators. By utilizing Wireless Local Area Network (WLAN) to carry LTE traffic, LWA is a palatable way to bring LTE and WLAN together [1], [2], [14]. LWA cleverly uses the well-established Wi-Fi protocols and coexistence mechanisms to carry LTE traffic to offer exceptionally fast data speeds. In 2017, we (Chunghwa Telecom) have deployed the first commercial LWA service in the world [3]. We also consider integrating LWA with mobile edge computing [20], [21] to enhance the radio bandwidth for edge computing.

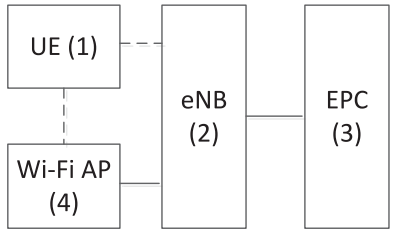


Fig. 1. A simplified LWA network architecture.

Fig. 1 illustrates a simplified LWA network architecture. The LWA-supported User Equipment (UE, Fig. 1 (1)) accesses the LTE network through the eNB (LTE base station; see Fig. 1 (2)), and sends packets to external networks through the Evolved Packet Core (EPC; see Fig. 1 (3)). To implement LWA, the Wi-Fi APs (Fig. 1 (4)) are connected to the eNB, and every downlink data stream from the EPC to the UE can be split at the eNB into two branches targeting at either LTE or WLAN.

One important issue about LWA is to detect the quality of WLAN, and provide the appropriate transmission rate to the UE. To maintain WLAN transmission quality such as low packet loss rates, the eNB adapts the transmission rate dynamically according to Wi-Fi AP's channel quality. To do so, 3GPP R13 [4], [6], [9], [15] has proposed two feedback mechanisms (which are followed by subsequent 3GPP releases): Xw-based feedback from the Wi-Fi AP and UE-based feedback from the UE. Since a typical legacy Wi-Fi AP does not provide Xw feedback, most studies consider the UE-based feedback mechanism. In [5], Lopez-Perez *et al*. used the periodical Packet Data Convergence Protocol (PDCP) LWA status report [6] to estimate the packet transmission delay over the WLAN channel. The delay over LTE channel can also be estimated by the Radio Link Control (RLC) status reports. Then the eNB sends the packet to the UE through the path with lower delay. However, this method may incur high

Manuscript received January 2, 2018; revised August 12, 2018; accepted August 13, 2018. Date of publication August 17, 2018; date of current version November 12, 2018. This work was supported in part by the Ministry of Science and Technology under Grants 106-2221-E-009-006 and 106-2221-E-009-049-MY2, in part by the Ministry of Education through the SPROUT Project-Center for Open Intelligent Connectivity of National Chiao Tung University, Taiwan, Academia Sinica AS-105-TP-A07, and in part by the Ministry of Economic Affairs 107-EC-17-A-24-1449 Taiwan. The review of this paper was coordinated by S. Zhang. *(Corresponding author: Yi-Bing Lin.)*

Y.-B. Lin is with the Department of Computer Science, National Chiao Tung University, Hsinchu 30010, Taiwan, R.O.C., and also with Chunghwa Telecom, Taipei 100, Taiwan, R.O.C. (e-mail: liny@cs.nctu.edu.tw).

Y.-J. Shih is with the Information and Communications Research Labs, Industrial Technology Research Institute, Hsinchu 31040, Taiwan, R.O.C., and also with the Department of Computer Science, National Chiao Tung University, Hsinchu 30010, Taiwan, R.O.C. (e-mail: yjshih.168@gmail.com).

H.-C. Tseng is with the Department of Computer Science, National Chiao Tung University, Hsinchu 30010, Taiwan, R.O.C. (e-mail: u9220043@gmail.com).

L.-J. Chen is with the Institute of Information Science, Academia Sinica, Taipei 115, Taiwan, R.O.C. (e-mail: ccljj@iis.sinica.edu.tw).

Digital Object Identifier 10.1109/TVT.2018.2865782

computing complexity because the eNB needs to estimate the transmission delay of each packet before transmission. In addition, this method may need to record the transmission path of each unacknowledged PDCP packet, which consumes extra system memory. In [7], Lin *et al*. proposed a simple scheme for the eNB to adapt the LTE to WLAN transmission ratio based on a predefined LTE-to-WLAN Ratio table. In this approach, the eNB estimates the WLAN channel quality based on the received WLAN signal strength index (RSSI) in the measurement reports periodically sent from the UE. The eNB then adapts the transmission rate based on the received RSSIs. This approach may waste the uplink radio resource and incur extra signaling load [8].

To resolve the above problems, we propose the enhanced event-triggered reporting approach. To the best of our knowledge, no researchers have proposed event-triggered reporting approach for LWA transmission rate adaption. In this approach, the UE sends a WLAN measurement report to the eNB only when it detects the RSSI change. Two pre-defined tables are built. The WLAN RSSI range table built in the UE consists of several WLAN RSSI ranges. The WLAN transmission rate table built in the eNB consists of several WLAN RSSI ranges (same as those saved in the UE) and their corresponding transmission rates. The UE triggers report sending according to the WLAN RSSI range table. Based on the received report, the eNB determines new transmission rate. As compared with periodical reporting, enhanced event-triggered reporting is optimal in the sense that it only generates necessary measurement report traffic. However, building the WLAN RSSI range table in the UE is not a trivial task. We will show that the table can be built without modifying the UE software. LWA is also affected by metrics such as system load and capacity of backhaul links. These metrics determine the upper bound transmission rate for downlink, and are typically used in network planning to select appropriate eNB and Wi-Fi APs. For example, if the backhaul link is 500 Mbps, then the operator will select the eNB and Wi-Fi APs such that the maximal net transmission rate is no more than 500 Mbps. Our approach is independently exercised without being affected by these metrics.

This paper is organized as follows. Section II describes WLAN RSSI measurement for switching APs (i.e., for mobility) based on the event-triggered mode, and for transmission rate adaption based on the periodical mode. We also point out potential problems of periodical reporting. Section III proposes enhanced event-triggered reporting for transmission rate adaption to mitigate the problems of periodical reporting. Section IV conducts analytic analysis to model periodical reporting. Section V uses the analytic results and measurements to validate the simulation experiments. Our study suggests how to select appropriate frequency to minimize the network traffic of periodical reporting. We also show that enhanced event-triggered reporting outperforms periodical reporting.

## II. WLAN RSSI Measurement Reporting

This section describes how WLAN RSSI measurement reports are used for UE mobility (i.e., switching between APs) and WLAN transmission rate adaption.

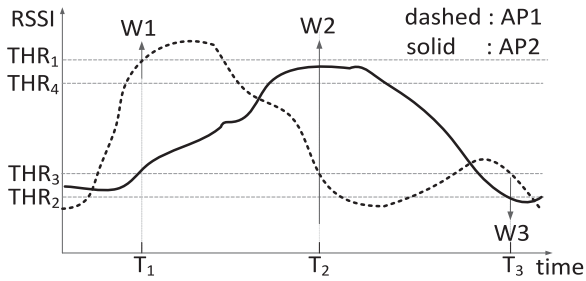


Fig. 2. Triggering for events W1, W2, and W3.

### A. Event-Triggered Reporting for UE Mobility

According to 3GPP TS 36.331 [9], the eNB can configure a UE to perform WLAN measurement and report the measurement results. There are 2 trigger modes of WLAN measurement reporting. Periodical reporting is typically used to adapt WLAN transmission rate of the serving Wi-Fi AP as we described in Section I. Event-triggered reporting is typically used in the mobility procedure to determine if the UE should connect to a Wi-Fi AP, switch to another AP or disconnect from the AP. When event-triggered reporting is configured, the UE sends a measurement report when one of three events occurs. Event W1 is triggered at a UE to notify the eNB only when LWA is not activated, and the UE detects a suitable Wi-Fi AP (i.e., the RSSI of the AP is better than a threshold $THR_1$). Then the eNB may activate LWA for the UE. Events W2 and W3 are triggered only when the UE is connected to a Wi-Fi AP (the serving AP). Event W2 is triggered if the RSSI of the serving AP becomes worse than a threshold $THR_3$ and the RSSI of a neighbor Wi-Fi AP becomes better than a threshold $THR_4$. Event W3 is triggered to notify the eNB that the RSSI of the serving AP becomes worse than a threshold $THR_2$, and the eNB may invoke the LWA deactivation procedure.

Fig. 2 depicts the RSSI changes of two Wi-Fi APs (AP 1 and AP 2) during an observation period. In the beginning, the UE is not connected to any AP. At $T_1$, the RSSI of the AP 1 becomes larger than $THR_1$. Therefore, the UE sends a W1-triggered (measurement) report to the eNB. The eNB then activates LWA by sending the LWA setup configuration to the UE. After successful WLAN association, AP 1 becomes the serving AP for the UE. At $T_2$, the RSSI of AP 1 drops below $THR_3$ and the RSSI of AP 2 is larger than $THR_4$. The UE sends a W2-triggered report to the eNB. The eNB then invokes the WLAN mobility procedure to transfer the UE from AP 1 to AP 2. When the RSSI of the serving AP 2 is smaller than $THR_2$, the UE sends a W3-triggered report to the eNB at $T_3$. Then the eNB sends the LWA release configuration to the UE, and LWA is deactivated after $T_3$.

In general, $THR_1 \geq THR_4 > THR_3 > THR_2$. From the above description, it is obvious that no event can trigger the UE to send a measurement report when the signal of the serving WLAN becomes better.

### B. Periodical Reporting for WLAN Transmission Rate Adaption

WLAN transmission rate adaption is performed at the Radio Resource Management layer (RRM) of the eNB. The RRM

TABLE I
WLAN TR TABLE

| WLAN RSSI Range | Transmission Rate |
|---|---|
| $\text{THR}_{\text{L1}}$ - INF | $\text{Rate}_1$ |
| $\text{THR}_{\text{L2}}$ - $\text{THR}_{\text{L1}}$ | $\text{Rate}_2$ |
| ….. | ….. |
| $\text{THR}_{\text{L}(m+1)}$ - $\text{THR}_{\text{L}m}$ | $\text{Rate}_{(m+1)}$ |
| ….. | ….. |
| $\text{THR}_{\text{L}M}$ -$\text{THR}_{\text{L}(M\text{-}1)}$ | $\text{Rate}_M$ |

uses a WLAN transmission rate table (TR; see Table I) to determine the transmission rate to the UE. In this table, $\text{THR}_{Lm} > \text{THR}_{L(m+1)}$ and $\text{Rate}_m > \text{Rate}_{m+1}$, where $1 \leq m < M$. Note that Infinity (INF)$\gg \text{THR}_{L1}$ represents a very large value. Also, $\text{THR}_{LM} = \text{THR}_2$ and $\text{THR}_{\text{L}(M-1)} > \text{THR}_1$.

Suppose that the UE sends a measurement report to the eNB with an RSSI such that $\text{THR}_{Lm} < \text{RSSI} < \text{THR}_{L(m-1)}$, then the RRM will instruct the PDCP layer to schedule the received packets and transmit them to the UE with the rate $\text{Rate}_m$. For the TR table used in the ITRI LWA eNB [7], $M = 6$, where $\text{THR}_{L1} = -50$ dBm, $\text{THR}_{L2} = -55$ dBm, $\text{THR}_{L3} = -60$ dBm, $\text{THR}_{L4} = -65$ dBm, $\text{THR}_{L5} = -70$ dBm, and $\text{THR}_{L6} = \text{THR}_2 = -75$ dBm. The transmission rates are $\text{Rate}_1 = 312$ Mbps, $\text{Rate}_2 = 248$ Mbps, $\text{Rate}_3 = 185$ Mbps, $\text{Rate}_4 = 156$ Mbps, $\text{Rate}_5 = 134$ Mbps, and $\text{Rate}_6 = 117$ Mbps, respectively.

When the UE is configured in the periodical reporting mode, it periodically sends the measurement reports, and the eNB uses the received RSSI to search the TR table to determine the transmission rate for the UE. Periodical reporting incurs two problems. First, the UE repeatedly sends the measurement reports to the eNB even if the RSSI does not change, which wastes the wireless bandwidth as well as computation resource at the eNB. This effect becomes serious if the reports are frequently sent. Second, the eNB cannot immediately detect the RSSI change until it receives the next report. This effect becomes serious if the reports are infrequently sent. We will investigate these two problems in Section IV.

A better way to detect the RSSI change is to download the first column of the TR table to the UE, and when the UE detects the RSSI change, it triggers to send the measurement report to the eNB. Unfortunately, the event-triggered reporting mechanism defined in 3GPP does not allow the UE to report the situation when the RSSI of the serving AP becomes better than a threshold (e.g., $\text{THR}_1$ in Fig. 2). In the next section, we propose a novel setup in event-triggered reporting to detect the situation when the RSSI of the serving AP becomes better.

## III. Enhanced Event-Triggered Reporting for Transmission Rate Adaption

From the description of event-triggered reporting, the events defined in the 3GPP LWA specifications cannot be used to adapt the transmission rate of the serving AP for the following reason. After the LWA is activated for a UE, there is no event to report when the serving AP's RSSI becomes better than a threshold. To resolve this issue, we propose a novel yet simple setting for Wi-Fi APs and the UE, which allows W2 to detect when the serving AP's RSSI becomes better. Our approach is called enhanced event-triggered reporting, which only slightly modify the RRM of the eNB.

In this approach, W2 is used to increase the transmission rate of the serving AP, and W3 is used to decrease the transmission rate. In WLAN, every Wi-Fi AP is identified by a service set identifier (SSID) and a basic service set identifier (BSSID). The idea is to configure every Wi-Fi AP in the LWA with two identities, where SSID1/BSSID1 is the serving AP identity (called the first identity) for normal LWA operations (activation, deactivation, mobility) and SSID2/BSSID2 is used as the identity to "pretend" that the serving AP is a neighbor AP. That is, SSID2/BSSID2 (called the second identity) is used to represent "AP 2" in Fig. 2 to trigger W2 for rate adaption at the serving AP. In the reminder of this section, we use AP 1 to represent the serving AP with the first identity, and AP 2 as the "neighbor AP", which is the serving AP with the second identity. Let $\text{RSSI}_x$ be the RSSI of AP $x$. Then $\text{RSSI}_1 = \text{RSSI}_2$ in our example.

Suppose that an LWA eNB physically connects to two APs, i.e., AP 1 and AP 3 where the first identity of AP 3 is SSID3/BSSID3. After a UE is connected to AP 1 with its first identity, the RSSI change rules are downloaded to the UE as follows. After LWA activation, the eNB sends the RRCConnectionReconfiguration message with the MeasConfig information element to the UE, which specifies the measurements to be performed by the UE. MeasConfig has 3 major parameters: measurement objects (MOs), reporting configurations (RCs) and measurement identities (MIs). An MO indicates the object (i.e., the AP specified by its identity) on which the UE will perform measurements. The format of an MO is "SSID/BSSID". In our example, there are three MOs, one for AP 1 (the serving AP), one for AP 2 (the serving AP pretending a neighbor AP), and one for AP 3 (the real neighbor AP). Therefore, the measObjectToAddModList element of MeasConfig includes the following MOs:

$$\mathbf{MO_1}\text{: }\mathbf{SSID1/BSSID1}, \mathbf{MO_2}\text{: }\mathbf{SSID2/BSSID2},$$
$$\mathbf{MO_3}\text{: }\mathbf{SSID3/BSSID3},$$

where $\text{MO}_1$ represents the first identity of AP 1, $\text{MO}_2$ represents the second identity of AP 1, and $\text{MO}_3$ represents the first identity of AP 3.

An RC specifies the reporting criteria such as the reporting trigger mode, the periodical reporting period, or the triggering conditions of an event. In our example, the reportingConfigToAddModList element of MeasConfig specifies $2M$ RCs, which implement the WLAN RSSI range table. The first $M-1$ RCs specify the W2 events for increasing the transmission rates:

$$\mathbf{RC_1}:\mathbf{W2}(\mathbf{INF}, \mathbf{THR_{L1}}), \mathbf{RC_2}:\mathbf{W2}(\mathbf{INF}, \mathbf{THR_{L2}}), \ldots,$$
$$\mathbf{RC}_{M-1}: \mathbf{W2}\left(\mathbf{INF}, \mathbf{THR}_{\mathbf{L}(M-1)}\right)$$

The $M$-th RC specifies the W2 event for switching from AP 1 to AP 3:

$$\mathbf{RC}_M: \mathbf{W2}(\mathbf{THR_3}, \mathbf{THR_4})$$

The next $M-1$ RCs specify the W3 events for decreasing the transmission rate:

$$\mathbf{RC_{M+1}}:\mathbf{W3}\left(\mathbf{THR_{L1}}\right),\mathbf{RC_{M+2}}:\mathbf{W3}\left(\mathbf{THR_{L2}}\right),\ldots,$$

$$\mathbf{RC_{2M-1}}:\mathbf{W3}\left(\mathbf{THR_{L}}_{(M-1)}\right)$$

and the last RC specifies the W3 event for LWA deactivation:

$$\mathbf{RC_{2M}}:\mathbf{W3}\left(\mathbf{THR_2}\right)$$

A measurement identity (MI) links an MO to an RC, which is included in the measurement report as a reference number of the measurement configuration. In our example, the MeasIdToAddModList element in MeasConfig configures $2M$ MIs, where the first $M-1$ of them specify the relationship between $\mathrm{MO}_2$ and $\mathrm{RC}_1-\mathrm{RC}_{M-1}$:

$$\mathbf{MI_1}:\left(\mathbf{MO_2},\mathbf{RC_1}\right),\mathbf{MI_2}:\left(\mathbf{MO_2},\mathbf{RC_2}\right),\ldots,$$

$$\mathbf{MI}_{\boldsymbol{M-1}}:\left(\mathbf{MO_2},\mathbf{RC}_{\boldsymbol{M-1}}\right),$$

For $1\le m\le M-1$, $\mathrm{MI}_m$ configures a W2 event to detect when to increase the WLAN transmission rate. Specifically, we set INF as the threshold for AP 1, and $\mathrm{THR}_{Lm}$ as the threshold for AP 2. When the serving AP's RSSI becomes larger than $\mathrm{THR}_{Lm}$ (i.e., $\mathrm{RSSI}_1=\mathrm{RSSI}_2\ge\mathrm{THR}_{Lm}$), this event is triggered because $\mathrm{RSSI}_1$ is always smaller than INF and $\mathrm{RSSI}_2\ge\mathrm{THR}_{Lm}$. Then the eNB uses $\mathrm{RSSI}_2$ to search the WLAN TR table, which results in selection of the transmission rate $\mathrm{Rate}_{m}$. The $M$-th MI links $\mathrm{MO}_3$ to $\mathrm{RC}_M$:

$$\mathbf{MI_M}:\left(\mathbf{MO_3},\mathbf{RC_M}\right)$$

When $\mathrm{RC}_M$ is met, it means that $\mathrm{RSSI}_1<\mathrm{THR}_3$ and $\mathrm{RSSI}_3>\mathrm{THR}_4$, and the eNB will switch AP 1 to AP 3. The last $M$ MIs link $\mathrm{MO}_1$ to $\mathrm{RC}_{M+1}-\mathrm{RC}_{2M}$:

$$\mathbf{MI}_{\boldsymbol{M+1}}:\left(\mathbf{MO_1},\mathbf{RC}_{\boldsymbol{M+1}}\right),\mathbf{MI}_{\boldsymbol{M+2}}$$

$$:\left(\mathbf{MO_1},\mathbf{RC}_{\boldsymbol{M+2}}\right),\ldots,$$

$$\mathbf{MI_{2M}}:\left(\mathbf{MO_1},\mathbf{RC_{2M}}\right)$$

For $1\le m\le M-1$, $\mathrm{MI}_{M+m}$ configures a W3 event to detect when to decrease the WLAN transmission rate. When $\mathrm{RC}_{M+m}$ $(1\le m<M)$ is met, $\mathrm{RSSI}_1<\mathrm{THR}_{Lm}$, and the eNB will selects the transmission rate $\mathrm{Rate}_{m+1}$. When $\mathrm{RC}_{2M}$ is met, $\mathrm{RSSI}_1<\mathrm{THR}_{LM}=\mathrm{THR}_2$, and eNB deactivates the UE from the LWA mode.

After the WLAN RSSI range table and the mobility criterion are established at the UE, it starts event-triggered reporting, and the eNB will receive one or more measurement reports triggered by the configured events. To support enhanced event-triggered reporting, the RRM of the eNB is slightly modified. First, when the MO of a W2 event is the second identity of AP 1, the RRM increases the transmission rate instead of switching the AP. Second, for a W3 event, if the received $\mathrm{RSSI}_1>\mathrm{THR}_2$, then the RRM decreases the transmission rate instead of deactivating LWA.

Note that our experiments as well as commercial operation do not use LTE signal strength to determine transmission rate because the variation of the LTE signal strengths is small. This is due to the fact that LTE utilizes the licensed band, which is seldom interfered by other base stations, and the pure LTE's throughput can be stably kept. On the other hand, the Wi-Fi RSSI dramatically changes from $-30$ dBm to $-75$ dBm [7]. Therefore, changing the LWA transmission data rate is based on the Wi-Fi RSSI value. If the LTE RSSI is not stable, we can also change the transmission rate via LTE based on the LTE RSSI strength.

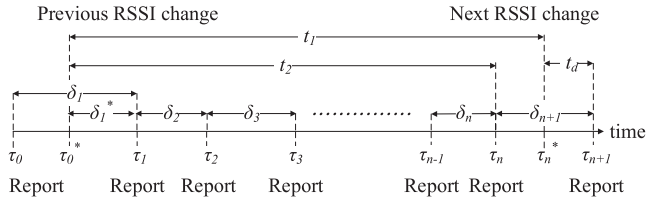


Fig. 3. The timing diagram for RSSI changes and the periodical reporting.

## IV. Modeling Periodical Reporting

Consider the timing diagram in Fig. 3. At time $\tau_0^*$ and $\tau_n^*$, the changes of the serving AP's RSSI measured by the UE are larger than a threshold. Therefore, when the eNB receives the WLAN measurement reports sent by the UE at $\tau_1$ and $\tau_{n+1}$, it changes the WLAN transmission rate based on the RSSI range table. Let $t_1=\tau_n^*-\tau_0^*$ be a random variable that represents the time interval between the previous RSSI change and the next RSSI change.

Assume that $t_1$ has the density function $f_1(t_1)$ and the Laplace Transform $f_1^*(s)=\int_{t_1=0}^{\infty}f_1(t_1)e^{-st_1}dt_1$. For $t_1$ with the Gamma distribution, we have

$$f_1\left(t_1\right)=f_1\left(t_1,\alpha,\beta\right)=\frac{\beta^{\alpha}{t_1}^{\alpha-1}e^{-\beta t_1}}{\Gamma\left(\alpha\right)} \tag{1}$$

where $\alpha$ is the shape parameter and $1/\beta$ is the scale parameter. The Gamma distribution is considered because it is widely used in modeling the transmission delay and cell residence times of moving UEs in telecommunications networks [10], [16]. From the statistics of commercial operation, we also found that the RSSI change can be appropriately modeled by a Gamma variable or a sum of Gamma variables. The Laplace transform of (1) is

$$f_1^*\left(s,\alpha,\ \beta\right)=\frac{\beta^{\alpha}}{\left(\mathrm{s}+\beta\right)^{\alpha}} \tag{2}$$

From the frequency-domain general derivative of Laplace transform, we have

$$\int_{t_1=\ 0}^{\infty}{t_1}^n f_1\left(t_1\right)e^{-st_1}dt_1=\left(-1\right)^n\left[\frac{f_1^{*(n)}\left(s\right)}{\mathrm{d}s^n}\right] \tag{3}$$

From (2) and (3), we have

$$\int_{t_1=0}^{\infty}{t_1}^n f_1\left(t_1,\alpha,\beta\right)e^{-st_1}dt_1=\frac{\Gamma\left(\alpha+n\right)\beta^{\alpha}}{\Gamma\left(\alpha\right)\left(\mathrm{s}+\beta\right)^{\alpha+n}} \tag{4}$$

Equations (2)–(4) will be used in the derivation of this section.

In Fig. 3, after the previous RSSI change occurs, the $i$-th measurement report is sent at $\tau_i$. For $i\ge1$, let $\delta_i=\tau_i-\tau_{i-1}$

represent the time interval between two measurement reports. A typical $\delta_i$ period is either a fixed interval or is Exponentially distributed. This section considers both cases.

### A. Exponential $\boldsymbol{\delta_i}$ and General $\boldsymbol{t}_1$

Let $\delta_i$ be i.i.d. random variables with the Exponential density function

$$f\ (\delta_i) = \gamma e^{-\gamma \delta_i} \tag{5}$$

Let random variable $N$ represent the number of measurement reports sent from the UE to the eNB between the previous RSSI change and the next RSSI change. For the derivation purpose, we express $\Pr[N\ =\ n]$ for an arbitrary $t_1$ distribution, and $\Pr[N\ =\ n, \alpha]$ for Gamma $t_1$ where $\alpha$ is the scale parameter in (1).

*Theorem 1:* For Exponentially distributed $\delta_i$, if $t_1$ has a general distribution, then

$$\Pr\left[N\ =\ n\right] = \left[\frac{(-\gamma)^n}{n!}\right]\left[\frac{f_1^{*(n)}\left(s\right)}{\mathrm{d}s^n}\right]\Bigg|_{s=\gamma}$$

For Gamma $t_1, \mathrm{E}\left[N\right] =\ \mathrm{E}[t_1]/\mathrm{E}[\delta_i]$.

*Proof:* Since $\delta_i$ is Exponentially distributed, for any interval $t_1$, $N$ has a Poisson distribution with the probability

$$\Pr\left[N\ =n,\ t_1\right] = \frac{(\gamma t_1)^n e^{-\gamma t_1}}{n!}$$

and

$$\begin{aligned}\Pr\left[N\ =\ n\right] &= \int_{t_1=0}^{\infty} \Pr\left[N=n,\ t_1\right] f_1\left(t_1\right) dt_1 \\ &= \left(\frac{\gamma^n}{n!}\right)\ \int_{t_1=\ 0}^{\infty} {t_1}^n f_1\left(t_1\right) e^{-\gamma t_1} dt_1 \end{aligned} \tag{6}$$

For $n \geq 0,$ substitute (3) into (6) to yield

$$\Pr\left[N\ =\ n\right] = \left[\frac{(-\gamma)^n}{n!}\right]\left[\frac{f_1^{*(n)}\left(s\right)}{\mathrm{d}s^n}\right]\Bigg|_{s=\gamma} \tag{7}$$

From (4), for Gamma $t_1$, we have

$$\begin{aligned}\Pr\left[N\ =\ n, \alpha\right] &= \frac{\beta^\alpha \gamma^n\ \Gamma\left(\alpha+n\right)}{\left(s+\beta\right)^{\alpha+n}\left(n!\right)\ \Gamma\left(\alpha\right)}\Bigg|_{s=\gamma} \\ &= \left[\frac{\Gamma\left(\alpha+n\right)}{\Gamma\left(\alpha\right)\left(n!\right)}\right]\ \left(\frac{\beta}{\gamma+\beta}\right)^\alpha \left(\frac{\gamma}{\gamma+\beta}\right)^n \end{aligned} \tag{8}$$

From either (7) or (8), we have

$$\Pr\left[N\ =\ 0, \alpha\right] = \left(\frac{\beta}{\gamma+\beta}\right)^\alpha \tag{9}$$

For Gamma $t_1$, the expected number $\mathrm{E}[N, \alpha]$ of the measurement reports between two RSSI changes is

$$\begin{aligned}\mathrm{E}\left[N, \alpha\right] &= \sum_{n=1}^{\infty} n\left[\frac{\Gamma\left(\alpha+n\right)}{\Gamma\left(\alpha\right)\left(n!\right)}\right]\left(\frac{\beta}{\gamma+\beta}\right)^\alpha \left(\frac{\gamma}{\gamma+\beta}\right)^n \\ &= \left[\frac{1}{\Gamma\left(\alpha\right)}\right]\left(\frac{\beta}{\gamma+\beta}\right)^\alpha \left\{\sum_{n\ =\ 1}^{\infty}\left[\frac{\Gamma\left(\alpha+n\right)}{(n-1)!}\right]\left(\frac{\gamma}{\gamma+\beta}\right)^n\right\} \\ &= \left[\frac{1}{\Gamma\left(\alpha\right)}\right]\ \left(\frac{\beta}{\gamma+\beta}\right)^\alpha \mathrm{S}\left(\alpha\right) \end{aligned} \tag{10}$$

where $\mathrm{S}\left(\alpha\right) = \sum_{n=1}^{\infty}[\frac{\Gamma(\alpha+n)}{(n-1)!}]x^n$ and $x\ = \frac{\gamma}{\gamma+\beta}$. We elaborate on $\mathrm{S}(\alpha)$ as

$$\begin{aligned}\mathrm{S}\ \left(\alpha\right) &= x\left\{\sum_{n\ =\ 1}^{\infty}\left[n\left(n+1\right)\cdots\left(n+\alpha-1\right)\right]x^{n-1}\right\} \\ &= x\left[\sum_{n\ =\ 1}^{\infty}\frac{d^\alpha}{dx^\alpha}\left(x^{n+\alpha-1}\right)\right] \\ &= x\left\{\frac{d^\alpha}{dx^\alpha}\left[\frac{1}{1-x} - \left(1+x+x^2+\cdots+x^{\alpha-1}\right)\right]\right\} \\ &= x\left\{\frac{d^\alpha}{dx^\alpha}\left[\frac{1}{1-x}\right]\right\} = \frac{\Gamma\left(\alpha+1\right)x}{\left(1-x\right)^{\alpha+1}} \\ &= \left\{\frac{\Gamma\left(\alpha+1\right)}{\left[1-\left(\frac{\gamma}{\gamma+\beta}\right)\right]^{\alpha+1}}\right\}\ \left(\frac{\gamma}{\gamma+\beta}\right) \end{aligned} \tag{11}$$

Substitute (11) into (10) to yield

$$\begin{aligned}\mathrm{E}\left[N, \alpha\right] &= \left[\frac{1}{\Gamma\left(\alpha\right)}\right]\ \left(\frac{\beta}{\gamma+\beta}\right)^\alpha \left[\frac{\Gamma\left(\alpha+1\right)\left(\frac{\gamma}{\gamma+\beta}\right)}{\left(1-\frac{\gamma}{\gamma+\beta}\right)^{\alpha+1}}\right] \\ &= \left[\frac{1}{\Gamma\left(\alpha\right)}\right]\ \left(\frac{\beta}{\gamma+\beta}\right)^\alpha \left[\frac{\Gamma\left(\alpha+1\right)\left(\frac{\gamma}{\gamma+\beta}\right)}{\left(\frac{\beta}{\gamma+\beta}\right)^{\alpha+1}}\right] \\ &= \frac{\alpha\left(\frac{\gamma}{\gamma+\beta}\right)}{\left(\frac{\beta}{\gamma+\beta}\right)}\ = \frac{\alpha\gamma}{\beta}\ = \frac{\mathrm{E}\left[t_1\right]}{\mathrm{E}\left[\delta_i\right]} \end{aligned}$$

which is independent of the variance of the $t_1$ distribution. **Q.E.D.**

In Fig. 3, $t_d = \delta_{n+1} - t_1 + t_2$. Now we prove that if $\delta_n$ is Exponentially distributed, then $t_d$ and $\delta_1^*$ have the same Exponential distribution.

*Theorem 2:* Suppose that $t_1 \geq \delta_1^*$. If $\delta_i$ is Exponentially distributed i.i.d. random variable, then for Gamma $t_1$ distribution, both $\delta_1^*$ and $t_d$ have the same distribution as $\delta_i$.

*Proof:* We prove by induction. In Fig. 3, we have $t_2 < t_1$ and $\delta_{n+1} + t_2 -\ t_1 = t_d\ > 0$. Let $t_{j,1}$ be the $t_1$ period for the $j$-th RSSI change, i.e., $t_{j,1}$ is the interval between the arrivals of the $j$-th RSSI and the $(j+1)$-th RSSI changes. Let $\delta_{j,1}^*$ be the $\delta_1^*$ period for the $j$-th RSSI change, $\delta_{j,i}$ be the $\delta_i$ period and $t_{j,d}$ be the $t_d$ period. Clearly, $t_{j,d}$ is $\delta_{j+1,1}^*$ for the $(j+1)$-th RSSI

change. Suppose that the hypothesis is true for the $(j-1)$-th RSSI change. That is, $\delta^*_{j,1}$ has the same Exponential distribution as $\delta_i$. Now we prove that the hypothesis is also true for the *j*-th RSSI change, i.e., $\delta^*_{j+1,1}$ $(t_{j,d})$ has the same distribution as $\delta_i$.

Let $f_d(t_{j,d})$ be the density function of $t_{j,d}$ under the condition that $N \geq 1$. That is, $t_{j,2} = \delta^*_{j,1} + \delta_{j,2} + \cdots + \delta_{j,n}$ and $t_{j,2} \leq t_{j,1} \leq t_{j,2} + t_{j,d}$. From the hypothesis, $\delta^*_{j,1}$ has the same Exponential distribution as $\delta_{j,1}$, and $t_{j,2}$ has the *n*-stage Erlang density function expressed as

$$f_2\ (t_{j,2}, n, \gamma) = \frac{\gamma^n {t_{j,2}}^{n-1} e^{-\gamma t_2}}{(n-1)!} \tag{12}$$

Let $f_d(t_{j,d}, n)$ be the density function of $t_{j,d}$ when $N = n \geq 1$. Then we have

$$f_d\ (t_{j,d}, n) = f_d\ (t_{j,d}) \Pr[N\ =\ n] \tag{13}$$

From (1), (5) and (12), $f_d(t_{j,d}, n)$ is expressed as

$$\begin{aligned} & f_d\left(t_{j,d}, n\right) \\ &= \int_{t_{j,1}=0}^{\infty} \int_{t_{j,2}=0}^{t_{j,1}} f_1\left(t_{j,1}\right) f_2(t_{j,2}, n, \gamma) f\left(t_{j,1} - t_{j,2} + t_{j,d}\right) dt_{j,2} dt_{j,1} \\ &= \gamma e^{-\gamma t_{j,d}} \int_{t_{j,1}=0}^{\infty} \int_{t_{j,2}=0}^{t_{j,1}} f_1\left(t_{j,1}\right) e^{-\gamma t_{j,1}} \left[\frac{\gamma^n {t_{j,2}}^{n-1}}{(n-1)!}\right] dt_{j,2} dt_{j,1} \\ &= \left(\frac{\gamma^{n+1} e^{-\gamma t_{j,d}}}{n!}\right) \int_{t_{j,1}=0}^{\infty} {t_{j,1}}^n f_1\left(t_{j,1}\right) e^{-\gamma t_{j,1}} dt_{j,1} \end{aligned} \tag{14}$$

Substitute (6) into (14) to yield

$$f_d\ (t_{j,d}, n) = \gamma e^{-\gamma t_{j,d}}\ \Pr[N\ =\ n, \alpha] \tag{15}$$

From (13) and (15), we have

$$f_d\ (t_{j,d}) =\ \gamma e^{-\gamma t_{j,d}} \tag{16}$$

Therefore, the hypothesis is true for $t_{j,d}$ $(\delta^*_{j+1,1})$. **Q.E.D.**

From (16), $\mathrm{E}[t_d, \alpha]$ is expressed as

$$\mathrm{E}\ [t_d, \alpha] = \int_{t_1=0}^{\infty} t_d f_d\ (t_d)\, dt_d = \quad \frac{1}{\gamma} = \mathrm{E}\left[\delta_i\right] \tag{17}$$

which is independent of the variance of the $t_1$ distribution.

We expect that when an RSSI change occurs, it is detected by the next measurement report with a delay $t_d$. If $t_d$ is large such that before the next measurement report arrives at the eNB, $J \geq 1$ RSSI changes occur. Then these measurement reports except for the last one are not detected, which will be investigated later. For an RSSI change, let $t'_d$ be $t_d$ such that $J\ =\ 0$, then the RSSI change is detected with the delay $t'_d$. We derive $\mathrm{E}[t'_d]$ as follows.

*Theorem 3:* If $\delta_i$ is Exponentially distributed, and $t_1$ has a general distribution. Then

$$\mathrm{E}\ [t'_d] = \frac{1}{\gamma}\ + \frac{\frac{f_1^*(s)}{\mathrm{d}s}\Big|_{s\ =\ \gamma}}{1 - f_1^*\ (\gamma)}$$

*Proof:* We note that $\mathrm{E}\ [t'_d] = \mathrm{E}[t_d | J\ =\ 0]$, where

$$\begin{aligned} & \mathrm{E}\left[t_d | J =\ 0\right] \Pr\ [J\ =\ 0] \\ &= \int_{t_1=0}^{\infty} \int_{t'_d=0}^{t_1} t'_d \gamma e^{-\gamma t'_d} f_1\left(t_1\right) dt'_d dt_1 \\ &= \int_{t_1=0}^{\infty} f_1\left(t_1\right) \left[\frac{1 - e^{-\gamma t_1} - \gamma t_1 e^{-\gamma t_1}}{\gamma}\right] dt_1 \\ &= \frac{1 - f_1^*\left(\gamma\right)}{\gamma}\ + \frac{f_1^{*(n)}\left(s\right)}{\mathrm{d}s}\Big|_{s=\gamma} \end{aligned} \tag{18}$$

The probability $\Pr[J\ =\ 0]$ is expressed as

$$\begin{aligned} \Pr\ [J\ =\ 0]\ &= \int_{t_1=0}^{\infty} \int_{t'_d=0}^{t_1} \gamma e^{-\gamma t'_d} f_1\left(t_1\right) dt'_d dt_1 \\ &=\ 1 - f_1^*\left(\gamma\right) \end{aligned} \tag{19}$$

Therefore, from (18) and (19), we have

$$\mathrm{E}\ [t'_d] = \mathrm{E}\ [t_d | J = 0] = \frac{1}{\gamma} + \frac{\frac{f_1^*(s)}{\mathrm{d}s}\Big|_{s=\gamma}}{1 - f_1^*\left(\gamma\right)} \tag{20}$$

**Q.E.D.**

From Theorem 2, (17) shows that $\mathrm{E}[t_d, \alpha]$ is independent of the $t_1$ distribution. On the other hand, from Theorem 3, (20) indicates that $\mathrm{E}[t'_d]$ is affected by the second and higher moments of the $t_1$ distribution.

When $N = 0$, $\delta_i > t_1$, and there may be more than $K$ RSSI changes occurring in $\delta_i$. Let $t_{1,k}$ be the $k$-th $t_1$ preiod in $\delta_i$, where $k \geq 1$. Note that the $\delta_i$ period starts at $\tau_i$, which is a random observer of $t_{1,1}$ . Let $t^*_{1,1}$ be the residual life of $t_{1,1,}$ and

$$T_{1,k}\ = t^*_{1,1}\ + \sum_{j\ =\ 2}^{k} t_{1,j} \tag{21}$$

For $k \geq 1$, let $\Pr[K \geq k, \alpha]$ be the probability that there are no less than $k$ RSSI changes in $\delta_i$. Then $\Pr[K \geq k, \alpha] = \Pr[\delta_i \geq T_{1,k}\ , \alpha]$ . Let $r_1(t^*_{1,1})$ be the density function of $t^*_{1,1}$. Then from (1) and the residual life theorem, we have

$$r_{1,1}\ (t^*_1) = \left\{\frac{1}{\mathrm{E}\left[t_1\right]}\right\}\ \left[1 - \int_0^{t^*_1} f_1\left(t^*_1\right) dt^*_1\right] \tag{22}$$

From (2), the Laplace transform of (22) is

$$r^*_{1,1}\ (s) = \left(\frac{1}{\mathrm{E}\left[t_1\right] s}\right)\ \left[1 - f_1^*\left(s\right)\right] \tag{23}$$

For $k \geq 1$, let $f_{1,k}(T_{1,k}\ )$ be the density function of $T_{1,k}$ . From (21), (2) and (23), and the convolution rule of the Laplace transform, $f^*_{1,k}(s)$ is

$$f^*_{1,k}\ (s) = \left(\frac{1}{\mathrm{E}\left[t_1\right] s}\right) \left[1 - f_1^*\left(s\right)\right] \left[f_1^*\left(s\right)\right]^{k-1} \tag{24}$$

We derive $\Pr[K\ =\ k]$ and $\mathrm{E}[K]$ as follows.

*Theorem 4:* If $\delta_i$ is Exponentially distributed, then for an arbitrary $t_1$ distribution,

$$\Pr[K=k] = \begin{cases} 1-\frac{\left[1-f_1^*(\gamma)\right]^2}{\mathrm{E}[t_1]\gamma} & \text{for } K=0 \\ \left(\frac{1}{\mathrm{E}[t_1]\gamma}\right)[1-f_1^*(\gamma)]^2[f_1^*(\gamma)]^{k-1} & \text{for } k\geq 1 \end{cases}$$

and $\mathrm{E}[K] = \mathrm{E}[\delta_i]/\mathrm{E}[t_1]$.

*Proof:* We first use (24) to derive $\Pr[K \geq k]$ as follows. Clearly, $\Pr[K \geq 0] = 1$. For $K \geq 1$, we have

$$\begin{aligned} \Pr[K\geq k] &= \int_{T_{1,k}=0}^{\infty}\int_{\delta_i=T_{1,k}}^{\infty} f_{1,k}(T_{1,k}) f(\delta_i)\, d\delta_i\, dT_{1,k} \\ &= \int_{T_{1,k}=0}^{\infty} f_{1,k}(T_{1,k}) e^{-\gamma T_{1,k}}\, dT_{1,k} \\ &= \left(\frac{1}{\mathrm{E}[t_1]\, s}\right)[1-f_1^*(s)][f_1^*(s)]^{k-1}\Big|_{s=\gamma} \\ &= \left(\frac{1}{\mathrm{E}[t_1]\,\gamma}\right)[1-f_1^*(\gamma)][f_1^*(\gamma)]^{k-1} \end{aligned} \tag{25}$$

$\Pr[K = k]$ can be directly derived as follows:

$$\Pr[K=k] = \Pr[K\geq k] - \Pr[K\geq k+1]$$

From (24), we have

$$\Pr[K=k] \tag{1}$$

$$= \begin{cases} 1-\frac{\left[1-f_1^*(\gamma)\right]^2}{\mathrm{E}[t_1]\gamma} & \text{for } K=0 \\ \left(\frac{1}{\mathrm{E}[t_1]\gamma}\right)[1-f_1^*(\gamma)]^2[f_1^*(\gamma)]^{k-1} & \text{for } k\geq 1 \end{cases} \tag{26}$$

If $t_1$ has the Gamma distribution, then (26) is rewritten as

$$\begin{aligned} \Pr[K=k,\alpha] = \left(\frac{\beta}{\alpha\gamma}\right)\left[1-\left(\frac{\beta}{\gamma+\beta}\right)^{\alpha}\right]^2 \\ \times\left(\frac{\beta}{\gamma+\beta}\right)^{(k-1)\alpha} \end{aligned} \tag{27}$$

The expected value of $K$ is expressed as

$$\begin{aligned} \mathrm{E}[K] &= \sum_{k=1}^{\infty}\left(\frac{k}{\mathrm{E}[t_1]\,\gamma}\right)[1-f_1^*(\gamma)]^2[f_1^*(\gamma)]^{k-1} \\ &= \left\{\frac{[1-f_1^*(\gamma)]^2}{\mathrm{E}[t_1]\,\gamma}\right\}\sum_{k=1}^{\infty} k[f_1^*(\gamma)]^{k-1} \\ &= \frac{1}{\mathrm{E}[t_1]\,\gamma} = \frac{\mathrm{E}[\delta_i]}{\mathrm{E}[t_1]} \end{aligned} \tag{28}$$

**Q.E.D.**

Equations (26) and (28) show that $\Pr[K = k]$ is affected by the $t_1$ distribution but $\mathrm{E}[K]$ is only affected by $\mathrm{E}[t_1]$.

### *B. General $\delta_i$ and Exponential $t_1$*

Let $\delta_i$ be i.i.d. random variables with a general density function $f(\delta_i)$ and $t_1$ has the Exponential density function

$$f_1(t_1) = f_1(t_1,1,\beta) = \beta e^{-\beta t_1}$$

Then the RSSI changes are random observers of the inter-arrival times $\delta_i$ of measurement reports. We derive $\Pr[K = k]$ and $\mathrm{E}[K]$ as follows.

*Theorem 5:* If $t_1$ is Exponentially distributed, then for an arbitrary $\delta_i$ distribution,

$$\Pr[K=k] = \left[\frac{(-\beta)^k}{k!}\right]\left[\frac{f^{*(k)}(s)}{ds^k}\right]\Big|_{s=\beta}$$

For a fixed $\delta_i$,

$$\Pr[K=k] = \frac{\left(\frac{\beta}{\gamma}\right)^k e^{-\frac{\beta}{\gamma}}}{k!}$$

and $\mathrm{E}[K] = \mathrm{E}[\delta_i]/\mathrm{E}[t_1]$.

*Proof:* Similar to the derivation for (6), the probability that there are $k$ RSSI changes between two measurement reports is

$$\Pr[K=k] = \left[\frac{(-\beta)^k}{k!}\right]\left[\frac{f^{*(k)}(s)}{ds^k}\right]\Big|_{s=\beta} \tag{29}$$

If $\delta_i$ is a fixed value, then its density function can be considered as a delayed delta function with the Laplace transform

$$f^*(s) = e^{-\frac{s}{\gamma}} \text{ and } \frac{df^{*(k)}(s)}{ds^k} = \left(-\frac{1}{\gamma}\right)^k e^{-\frac{s}{\gamma}}$$

Therefore, (29) is rewritten as

$$\Pr[K=k] = \frac{\left(\frac{\beta}{\gamma}\right)^k e^{-\frac{\beta}{\gamma}}}{k!} \tag{30}$$

and

$$\mathrm{E}[K] = \frac{\beta}{\gamma} = \frac{\mathrm{E}[\delta_i]}{\mathrm{E}[t_1]} \tag{31}$$

**Q.E.D.**

The $t_d$ density function, $\mathrm{E}[t_d]$ and $\mathrm{E}[t_d']$ are derived as follows.

*Theorem 6:* If $t_1$ is Exponentially distributed, then for a fixed $\delta_i$,

$$\mathrm{E}[t_d'] = \frac{1}{\beta} - \left(\frac{1}{\gamma}\right)\left(\frac{e^{-\frac{\beta}{\gamma}}}{1-e^{-\frac{\beta}{\gamma}}}\right)$$

*Proof:* Since $t_1$ is Exponentially distributed, the RSSI changes are random observers of $\delta_i$. From (22)

$$f_d(t_d) = \left\{\frac{1}{\mathrm{E}[\delta_i]}\right\}\left[1-\int_0^{t_d} f(t_d)\, dt_d\right] \tag{32}$$

For a fixed $\delta_i$, (32) is rewritten as

$$f_d(t_d) = \begin{cases} \gamma & \text{for } 0\leq t_d\leq \frac{1}{\gamma} \\ 0 & \text{for } t_d \geq \frac{1}{\gamma} \end{cases}$$

and

$$\mathrm{E}[t_d] = \int_{t_d=0}^{\frac{1}{\gamma}} t_d f_d(t_d) dt_d = \frac{1}{2\gamma} \tag{33}$$

Now we derive $\mathrm{E}[t'_d]$ as follows.

$$\mathrm{E}\left[t'_d|J\ =\ 0\right]\Pr\left[J\ =\ 0\right]\ =\ \int_{t'_d=0}^{\frac{1}{\gamma}}\int_{t_1=t'_d}^{\infty}\beta t'_d e^{-\beta t_1}\gamma dt'_d dt_1$$
$$=\int_{t'_d=0}^{\frac{1}{\gamma}}\gamma t'_d e^{-\beta t'_d}\,dt'_d$$
$$=\frac{\gamma\left(1-e^{-\frac{\beta}{\gamma}}-\frac{\beta}{\gamma}e^{-\frac{\beta}{\gamma}}\right)}{\beta^2} \qquad (34)$$

and

$$\Pr\ [J\ =\ 0]\ =\int_{t'_d=0}^{\frac{1}{\gamma}}\int_{t_1=t'_d}^{\infty}\beta e^{-\beta t_1}\gamma dt'_d dt_1$$
$$=\int_{t'_d=0}^{\frac{1}{\gamma}}\gamma e^{-\beta t'_d}\,dt'_d\ =\left(\frac{\gamma}{\beta}\right)\left(1-e^{-\frac{\beta}{\gamma}}\right) \qquad (35)$$

Therefore, from (34) and (35)

$$\mathrm{E}\ [t'_d]=\ \mathrm{E}\left[t_d|J\ =\ 0\right]$$
$$=\left[\frac{\gamma\left(1-e^{-\frac{\beta}{\gamma}}-\frac{\beta}{\gamma}e^{-\frac{\beta}{\gamma}}\right)}{\beta^2}\right]\left[\left(\frac{\gamma}{\beta}\right)\left(1-e^{-\frac{\beta}{\gamma}}\right)\right]^{-1} \qquad (36)$$
$$=\frac{1}{\beta}\ -\left(\frac{1}{\gamma}\right)\left(\frac{e^{-\frac{\beta}{\gamma}}}{1-e^{-\frac{\beta}{\gamma}}}\right)$$

**Q.E.D.**

Now we derive $\Pr[N\ =\ n]$ and $\mathrm{E}[N]$.

*Theorem 7:* If $t_1$ is Exponentially distributed, then for an arbitrary $\delta_i$ distribution,

$$\Pr\left[N\ =\ n\right]=\left(\frac{1}{\mathrm{E}\left[\delta_i\right]\beta}\right)\left[1-f^*\left(\beta\right)\right]^2\left[f^*\left(\beta\right)\right]^{n-1}$$

and for a fixed $\delta_i, \mathrm{E}[N]=\ \mathrm{E}[t_1]/\mathrm{E}[\delta_i]$.

*Proof:* If $N\ =\ n\geq 1$, then the Laplace Transform of the $t_2$ distribution is

$$f_2^*\ (s)=\left(\frac{1}{\mathrm{E}\left[\delta_i\right]s}\right)\left[1-f^*\left(s\right)\right]\left[f^*\left(s\right)\right]^{n-1} \qquad (37)$$

From (37)

$$\Pr\left[N\geq n\right]\ =\int_{t_2=0}^{\infty}\int_{t_1=t_2}^{\infty}f_1\left(t_1\ \right)f_2\left(t_2\ \right)dt_1\ dt_2$$
$$=\left(\frac{1}{\mathrm{E}\left[\delta_i\right]\beta}\right)\left[1-f^*\left(\beta\right)\right]\left[f^*\left(\beta\right)\right]^{n-1} \qquad (38)$$

Therefore, $\Pr[N\ =\ n]$ is derived from (38) as

$$\Pr\left[N\ =\ n\right]=\left(\frac{1}{\mathrm{E}\left[\delta_i\right]\beta}\right)\left[1-f^*\left(\beta\right)\right]^2\left[f^*\left(\beta\right)\right]^{n-1} \qquad (39)$$

If $\delta_i$ is a fixed value, then for $n>0$,

$$\Pr\left[N\ =\ n\right]=\left(\frac{\gamma}{\beta}\right)\ \left[1-e^{-\frac{\beta}{\gamma}}\right]^2 e^{-\frac{(n-1)\beta}{\gamma}} \qquad (40)$$

and

$$\mathrm{E}\left[N\right]=\frac{\gamma}{\beta}\ =\frac{\mathrm{E}\left[t_1\right]}{\mathrm{E}\left[\delta_i\right]} \qquad (41)$$

**Q.E.D.**

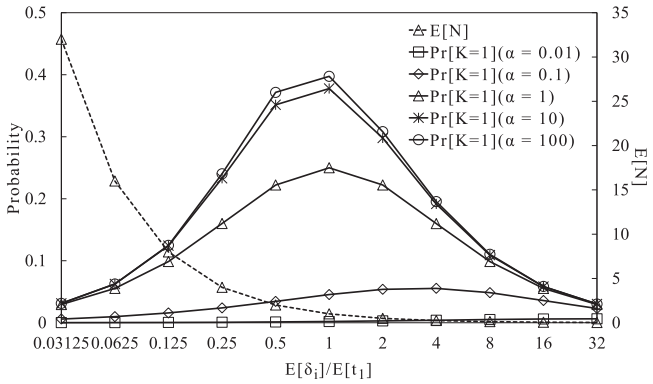


(a) Exponential $\delta_i$

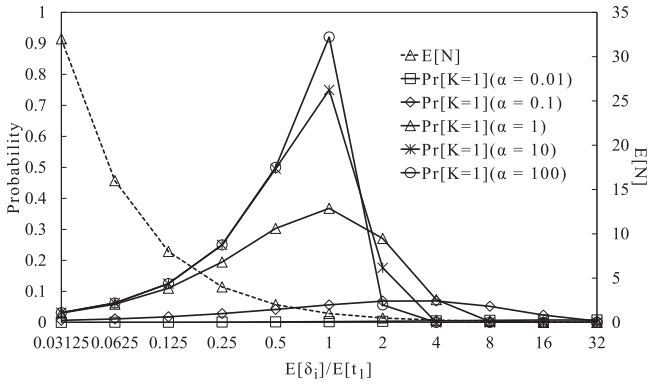


(b) Fixed $\delta_i$

Fig. 4. $\Pr[K\ =\ 1]$ and E[ $N$] against $\delta_i$.

Equations (39) and (40) show that $\mathrm{E}[N]$ is independent of the variance and higher moments of the $\delta_i$ distribution, while $\Pr[N\ =\ n]$ is affected by the $\delta_i$ distribution.

## V. Performance Evaluation

We have actually implemented periodical reporting and enhanced event-triggered reporting in the ITRI eNB. This section conducts simulation experiments and measurements of ITRI eNB to investigate the performance of both periodical and event-triggered reporting. The analytic analysis described in Section IV is partially validated by the measurements. The simulation methodology can be found in [11]–[13], and the simulation experiments are validated by both analytic analysis and the measurements. For $\Pr[K=1]$, $\mathrm{E}[t'_d]$ and $\mathrm{E}[N]$, the discrepancies between the simulation experiments and the analytic analysis are less than 0.07% for Exponential $\delta_i$ and 0.06% for fixed $\delta_i$. In [7], the UE is configured with fixed $\delta_i=$ 1024 ms, and E[ $t_1$] = 5 seconds. In the measurements, we obtain $\mathrm{E}[N]=\ 4.870$. The analytic result computed by using Equation (41) is $\mathrm{E}[N]=\ 4.883$, which is consistent with the measurement.

To achieve good performance, the $\delta_i$ value should be chosen such that $\mathrm{E}[N]$ is small, $\mathrm{E}[t'_d]$ is small, and $\Pr[K=1]$ is large. Figs. 4 and 5 show the performance of these output measures for periodical reporting. In these figures, $t'_d$ and $\delta_i$ are normalized by E[ $t_1$], where $t_1$ has the Gamma distribution with different variances, and $\delta_i$ is either fixed or

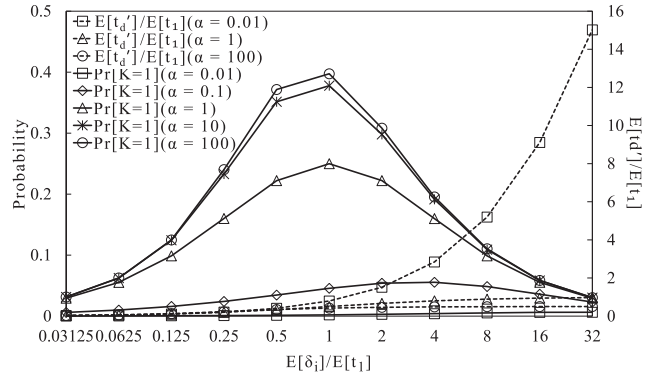


(a) Exponential $\delta_i$

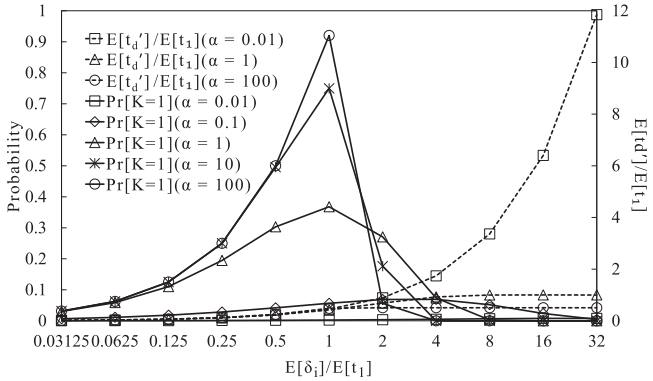


(b) Fixed $\delta_i$

Fig. 5. $\Pr[K=1]$ and $\mathrm{E}[t'_d]$ against $\delta_i$.

Exponentially distributed. Fig. 4 plots the $\mathrm{E}[N]$ and the $\Pr[K=1]$ curves against $\mathrm{E}[\delta_i]$ (normalized by E[ $t_1$]). The figure shows that when $\mathrm{E}[\delta_i]$ increases, $\Pr[K=1]$ increases and then decreases. When $\delta_i$ is small, it is likely that $K=0$. Therefore, increasing $\delta_i$ will decrease $\Pr[K=0]$ and the probability that $K=1$ increases. When $\delta_i$ is large, it is likely that more than one RSSI changes occur in a $\delta_i$ period. Therefore, increasing $\delta_i$ will decrease $\Pr[K=1]$. The maximal $\Pr[K=1]$ occurs when $\mathrm{E}[\delta_i] \approx \mathrm{E}[t_1]$.

We also observe that $\Pr[K=1]$ decreases as $\alpha$ decreases (the variance of the $t_1$ distribution increases). When the variance of $t_1$ increases, there are more short $t_1$ periods (where $K=0$) and more very long $t_1$ periods (where $K \geq 2$), and $\Pr[K=1]$ decreases. When $\alpha \geq 1$, the maximal $\Pr[K=1]$ occurs at $\mathrm{E}[\delta_i] \approx \mathrm{E}[t_1]$. When $\alpha < 1$, the maximal $\Pr[K=1]$ occurs when $\mathrm{E}[\delta_i] > \mathrm{E}[t_1]$.

From Theorems 1 and 7, $\mathrm{E}[N]$ is a decreasing function of $\mathrm{E}[\delta_i]$. The non-trivial result is that when $\mathrm{E}[\delta_i] \leq \mathrm{E}[t_1]$, $\mathrm{E}[N]$ significantly decreases as $\mathrm{E}[\delta_i]$ increases. On the other hand, when $\mathrm{E}[\delta_i] > \mathrm{E}[t_1]$, $\mathrm{E}[N]$ is insignificantly affected by $\mathrm{E}[\delta_i]$.

In periodical reporting, we should select $\mathrm{E}[\delta_i]$ such that $\mathrm{E}[N]$ is small and $\Pr[K=1]$ is large. From the curves in Fig. 4, $\mathrm{E}[\delta_i] \approx \mathrm{E}[t_1]$ should be chosen so that $\Pr[K=1]$ is maximized and $\mathrm{E}[N]$ is sufficiently small.

Fig. 5 shows that $\mathrm{E}[t'_d]$ increases as $\delta_i$ increases. When $\mathrm{E}[\delta_i] \leq \mathrm{E}[t_1]$, $\mathrm{E}[t'_d]$ insignificantly increases as $\mathrm{E}[\delta_i]$ increases. When $\mathrm{E}[\delta_i] > \mathrm{E}[t_1]$, $\mathrm{E}[t'_d]$ is more significantly affected by $\mathrm{E}[\delta_i]$. We also observe that $\mathrm{E}[t'_d]$ decreases as $\alpha$ decreases (the variance of $t_1$ increases). When the variance of the $t_1$ distribution increases, much more short $t_1$ than long $t_1$, and more $t_1$ will fall in a $\delta_i$ period, which results in a smaller $t'_d$. In periodical reporting, we should select $\mathrm{E}[\delta_i]$ such that $\mathrm{E}[t'_d]$ is small and $\Pr[K=1]$ is large. Based on our observation in Fig. 5, $\mathrm{E}[\delta_i] \approx \mathrm{E}[t_1]$ should be chosen.

For $\mathrm{E}[N]$, both Exponential and fixed $\delta_i$ have the same performance. When $\mathrm{E}[\delta_i]/\mathrm{E}[t_1] < 2, \Pr[K=1]$ for fixed $\delta_i$ is larger than Exponential $\delta_i$. On the other hand, when $\mathrm{E}[\delta_i]/\mathrm{E}[t_1] > 2$, the result reverses. When $\mathrm{E}[\delta_i]/\mathrm{E}[t_1] < 2, \mathrm{E}[t'_d]$, for fixed $\delta_i$ is smaller than Exponential $\delta_i$. On the other hand, when $\mathrm{E}[\delta_i]/\mathrm{E}[t_1] > 2$, the result reverses. The above results show that when $\mathrm{E}[\delta_i]/\mathrm{E}[t_1]$ is small, fixed $\delta_i$ yields better performance and should be selected; otherwise, Exponential $\delta_i$ should be selected.

Based on the above discussion about Fig. 5, $\mathrm{E}[\delta_i] \approx \mathrm{E}[t_1]$ should be chosen so that $\Pr[K=1]$ is maximized and $\mathrm{E}[t'_d]$ is sufficiently small. For Exponential $\delta_i$, when $\alpha = 1$ and $\mathrm{E}[\delta_i] = \mathrm{E}[t_1]$, we have $\Pr[K=1] = 0.249958$, $\mathrm{E}[N] = 1.00066$, and $\mathrm{E}[t'_d] = 0.49995\mathrm{E}[\delta_i]$. When $\alpha = 100, \Pr[K=1] = 0.397383$, $\mathrm{E}[N] = 0.999684$, and $\mathrm{E}[t'_d] = 0.419364\mathrm{E}[\delta_i]$. For fixed $\delta_i$, when $\alpha = 1$, and $\mathrm{E}[\delta_i] = \mathrm{E}[t_1]$, we have $\Pr[K=1] = 0.367938, \mathrm{E}[N] = 1.00024$, and $\mathrm{E}[t'_d] = 0.418015\mathrm{E}[\delta_i]$. When $\alpha = 100, \Pr[K=1] = 0.920444, \mathrm{E}[N] = 0.999979$, and $\mathrm{E}[t'_d] = 0.481936\mathrm{E}[\delta_i]$.

In enhanced event-triggered reporting, $\Pr[K=1] = 1$, $t'_d = 0$, and $N = 1$, which is optimal as compared with periodical reporting. When $\alpha = 1$ and $\mathrm{E}[\delta_i] = \mathrm{E}[t_1]$, the event triggered reporting can save 36% redundant measurement reports and increase the accuracy of the RSSI change detection by 26% without RSSI change detection delay. In our approach, an extra overhead comes from using fake neighbor AP. The Wi-Fi bandwidth consumed by the fake neighbor is about 1.121% [17]. This overhead is small and acceptable in commercial operation. As for downloading the triggering rules, it is merely a one-time overhead. We have conducted experiments to measure the message exchange time of the RRC Connection Reconfiguration message pair for the measurement configuration (the time between when the eNB RRM issues "RRCConnectionReconfiguration" message and when the UE reports "RRCConnectionReconfigurationComplete" message). The average time of 1000 measurements is 37.7058 ms when $M = 1$ (i.e., no enhanced event-triggered reporting) and 38.414916 ms when $M = 6$. Our measurements indicate the enhanced event-triggered reporting incurs negligible overhead.

## VI. Conclusion

LWA utilizes periodical reporting to adapt the WLAN transmission rate. How to select an appropriate period for sending measurement reports is an important issue that will affect the LWA performance. In this paper, we conducted the measurements, analytic analysis and the simulation experiments to provide guidelines for selection of appropriate frequency to minimize the network traffic of periodical reporting.

We then proposed enhanced event-triggered reporting, a novel approach to enhance 3GPP event-triggered reporting to

increase/decrease the WLAN transmission rate. This approach fully explores the LWA transmission capacity by detecting the WLAN radio bandwidth in real time. We showed that enhanced event-triggered reporting incurs little extra overhead, and therefore outperforms periodical reporting. Our solution utilizes the standard 3GPP protocols and does not modify the mobile phone's software. This work is pending US, China and Taiwan patents. In the future, we will investigate the event-triggered reporting method in the dense network. For example, we can use reporting events to request the UE to report the nearby Wi-Fi AP in the same and adjacent frequency channels to detect congestion. We will also investigate the LWA rate adaption when LTE signal is unstable.

## REFERENCES


[1] P. Nuggehalli, "LTE-WLAN aggregation," *IEEE Wireless Commun.*, vol. 23, no. 4, pp. 4–6, Aug. 2016.

[2] S. Sirotkin, "LTE-wireless aggregation (LWA): Benefits and deployment considerations," Intel White Paper, 2017.

[3] Y.-K. Tu, C.-H. Lee, C.-H. Liu, C.-Y. Chia, Y.-K. Chen, and Y.-B. Lin, "Deployment of the first commercial LWA service," *IEEE Wireless Commun.*, vol. 24, no. 6, pp. 6–8, Dec. 2017.

[4] *Evolved Universal Terrestrial Radio Access (E-UTRA) and Wireless LAN (WLAN); XW Application Protocol (Release 13)*, 3GPP TS 36.463, V13.0.0, Mar. 2016.

[5] D. Lopez-perez *et al.*, "Long term evolution-wireless local area network aggregation flow control," *IEEE Access*, vol. 4, pp. 9860–9869, Jan. 2017.

[6] *Evolved Universal Terrestrial Radio Access (E-UTRA); Packet Data Convergence Protocol (PDCP) Specification (Release 13)*, 3GPP TS 36.323, V13.1.0, Mar. 2016.

[7] Y.-B. Lin, H.-C. Tseng, L.-C. Wang, and L.-J. Chen, "Performance of splitting LTE-WLAN aggregation," *Mobile Netw. Appl.*, 2018.

[8] K. Hiltunen, N. Binucci, and J. Bergstrom, "Comparison between the periodic and event-triggered intra-frequency handover measurement reporting in WCDMA," in *Proc. IEEE Wirel. Commun. Netw. Conf.*, 2000, pp. 471–475.

[9] *Evolved Universal Terrestrial Radio Access (E-UTRA); Radio Resource Control (RRC) Protocol Specification (Release 13)*, 3GPP TS 36.331, V13.1.0, Mar. 2016.

[10] Y.-B. Lin and A.-C. Pang, *Wireless and Mobile All-IP Networks*. Hoboken, NJ, USA: Wiley 2005.

[11] C.-Y. Hong and A.-C. Pang, "3-approximation algorithm for joint routing and link scheduling in wireless relay networks," *IEEE Trans. Wireless Commun.*, vol. 8, no. 2, pp. 856–861, Feb. 2009.

[12] D.-W. Huang, P. Lin, and C.-H. Gan, "Design and performance study for a mobility management mechanism (WMM) using location cache for wireless mesh network," *IEEE Trans. Mobile Comput.*, vol. 7, no. 5, pp. 546–556, May 2008.

[13] S. Y. Tsai, S. I. Sou, and M. H. Tsai, "Reducing energy consumption by data aggregation in M2M networks," *Wireless Pers. Commun.*, vol. 74, no. 4, pp. 1231–1244, Feb. 2014.

[14] Y.-B. Lin, Y.-J. Shih, and P.-W. Chao, "Design and implementation of LTE RRM with switched LWA policies," *IEEE Trans. Veh. Technol.*, vol. 67, no. 2, pp. 1053–1062, Feb. 2018.

[15] *Evolved Universal Terrestrial Radio Access (E-UTRA) and Evolved Universal Terrestrial Radio Access Network (E-UTRAN); Overall Description; Stage 2 (Release 13)*, 3GPP TS 36.300, V13.4.0, Jun. 2016.

[16] M. M. Zonoozi and P. Dassanayake, "User mobility modeling and characterization of mobility patterns," *IEEE J. Sel. Areas Commun.*, vol. 15, no. 5, pp. 1239–1252, Sep. 1997.

[17] Aruba networks, "Improve air quality by minimizing SSIDs: Using role-based access to increase Wi-Fi application performance," Oct. 2010. [Online]. Available: https://www.arubanetworks.com/pdf/technology/whitepapers/wp_Virtual-Access-Points.pdf

[18] J. Liu, H. Nishiyama, N. Kato, and J. Guo, "On the outage probability of device-to-device-communication-enabled multichannel cellular networks: An RSS-threshold-based perspective," *IEEE J. Sel. Areas Commun.*, vol. 34, no. 1, pp. 163–175, Jan. 2016.

[19] J. Gao, L. Zhao, and X. Shen, "Network utility maximization based on incentive mechanism for truthful reporting of local information," *IEEE Trans. Veh. Technol.*, vol. 67, no. 8, pp. 7523–7537, Aug. 2018.

[20] T. G. Rodrigues, K. Suto, H. Nishiyama, and N. Kato, "Hybrid method for minimizing service delay in edge cloud computing through VM migration and transmission power control," *IEEE Trans. Comput.*, vol. 66, no. 5, pp. 810–819, May 2017.

[21] T. G. Rodrigues, K. Suto, H. Nishiyama, N. Kato, and K. Temma, "Cloudlets activation scheme for scalable mobile edge computing with transmission power control and virtual machine migration," *IEEE Trans. Comput.*, vol. 67, no. 9, pp. 1287–1300, Sep. 2018.

[22] S. Han, Y.-C. Liang, Q. Chen, and B.-H. Soong, "Licensed-assisted access for LTE in unlicensed spectrum: A MAC protocol design," *IEEE J. Sel. Areas Commun.*, vol. 34, no. 10, pp. 2550–2561, Oct. 2016.


**Yi-Bing Lin** (M'96–SM'96–F'03) is the Vice Chancellor with the University System of Taiwan, and the Lifetime Chair Professor with the National Chiao Tung University. During 2014–2016, he was a Deputy Minister of the Ministry of Science and Technology, Taiwan. He is also an Adjunct Research Fellow with the Institute of Information Science, and Center for Information Technology Innovation, Academia Sinica, and a member of board of directors, Chunghwa Telecom. He has authored several books: *Wireless and Mobile Network Architecture* (Wiley, 2001), *Wireless and Mobile All-IP Networks* (Wiley, 2005), and *Charging for Mobile All-IP Telecommunications* (Wiley, 2008). He was the recipient of the TWAS Prize in Engineering Sciences in 2011 (The World Academy of Sciences). He serves as the Chair of IEEE Taipei Section. He is an AAAS Fellow, an ACM Fellow, and an IET Fellow.

**Ying-Ju Shih** received the B.S. degree in electrical engineering and the M.S. degree in communication engineering both from the National Tsing Hua University, Hsinchu, Taiwan, in 2001 and 2003, respectively. She is currently working toward the Ph.D. degree in computer science at the National Chiao Tung University, Hsinchu. Since 2013, she has been an Engineer with the Information and Communications Research Labs, Industrial Technology Research Institute, Hsinchu. Her current research interests include heterogeneous wireless communication systems and Internet of things.

**Hung-Chun Tseng** received the B.S. degree from National Hsinchu University of Education, Hsinchu, Taiwan, in 2007, and the M.S. degree from National Chiao Tung University (NCTU), Hsinchu, in 2011. He is currently working toward the Ph.D. degree at the Department of Computer Science, NCTU.

**Ling-Jyh Chen** (S'03–M'05–SM'12) received the B.Ed. degree in information and computer education from National Taiwan Normal University Taipei, Taiwan, in 1998, and the M.S. and Ph.D. degrees in computer science from the University of California, Los Angeles, CA, USA, in 2002 and 2005, respectively. He joined the Institute of Information Science of Academia Sinica as an Assistant Research Fellow in 2005, and became an Associate Research Fellow in 2011. His research interests include networked sensing systems, network measurements, and mobile data management. He is a senior member of the IEEE.